

Study of τ Decays to Six Pions and a Neutrino

A. Anastassov,¹ J. E. Duboscq,¹ E. Eckhart,¹ K. K. Gan,¹ C. Gwon,¹ T. Hart,¹ K. Honscheid,¹ D. Hufnagel,¹ H. Kagan,¹ R. Kass,¹ T. K. Pedlar,¹ H. Schwarthoff,¹ J. B. Thayer,¹ E. von Toerne,¹ M. M. Zoeller,¹ S. J. Richichi,² H. Severini,² P. Skubic,² A. Undrus,² S. Chen,³ J. Fast,³ J. W. Hinson,³ J. Lee,³ D. H. Miller,³ E. I. Shibata,³ I. P. J. Shipsey,³ V. Pavlunin,³ D. Cronin-Hennessy,⁴ A. L. Lyon,⁴ E. H. Thorndike,⁴ C. P. Jessop,⁵ V. Savinov,⁵ T. E. Coan,⁶ V. Fadeyev,⁶ Y. Maravin,⁶ I. Narsky,⁶ R. Stroynowski,⁶ J. Ye,⁶ T. Wlodek,⁶ M. Artuso,⁷ R. Ayad,⁷ C. Boulahouache,⁷ K. Bukin,⁷ E. Dambasuren,⁷ S. Karamov,⁷ G. Majumder,⁷ G. C. Moneti,⁷ R. Mountain,⁷ S. Schuh,⁷ T. Skwarnicki,⁷ S. Stone,⁷ G. Viehhauser,⁷ J. C. Wang,⁷ A. Wolf,⁷ J. Wu,⁷ S. Kopp,⁸ A. H. Mahmood,⁹ S. E. Csorna,¹⁰ I. Danko,¹⁰ K. W. McLean,¹⁰ Z. Xu,¹⁰ R. Godang,¹¹ G. Bonvicini,¹² D. Cinabro,¹² M. Dubrovin,¹² S. McGee,¹² G. J. Zhou,¹² E. Lipeles,¹³ S. P. Pappas,¹³ M. Schmidtler,¹³ A. Shapiro,¹³ W. M. Sun,¹³ A. J. Weinstein,¹³ F. Würthwein,^{13,*} D. E. Jaffe,¹⁴ G. Masek,¹⁴ H. P. Paar,¹⁴ E. M. Potter,¹⁴ S. Prell,¹⁴ D. M. Asner,¹⁵ A. Eppich,¹⁵ T. S. Hill,¹⁵ R. J. Morrison,¹⁵ R. A. Briere,¹⁶ G. P. Chen,¹⁶ W. T. Ford,¹⁷ A. Gritsan,¹⁷ J. Roy,¹⁷ J. G. Smith,¹⁷ J. P. Alexander,¹⁸ R. Baker,¹⁸ C. Bebek,¹⁸ B. E. Berger,¹⁸ K. Berkelman,¹⁸ F. Blanc,¹⁸ V. Boisvert,¹⁸ D. G. Cassel,¹⁸ P. S. Drell,¹⁸ K. M. Ecklund,¹⁸ R. Ehrlich,¹⁸ A. D. Folland,¹⁸ P. Gaidarev,¹⁸ R. S. Galik,¹⁸ L. Gibbons,¹⁸ B. Gittelman,¹⁸ S. W. Gray,¹⁸ D. L. Hartill,¹⁸ B. K. Heltsley,¹⁸ P. I. Hopman,¹⁸ L. Hsu,¹⁸ C. D. Jones,¹⁸ D. L. Kreinick,¹⁸ M. Lohner,¹⁸ A. Magerkurth,¹⁸ T. O. Meyer,¹⁸ N. B. Mistry,¹⁸ E. Nordberg,¹⁸ J. R. Patterson,¹⁸ D. Peterson,¹⁸ D. Riley,¹⁸ A. Romano,¹⁸ J. G. Thayer,¹⁸ D. Urner,¹⁸ B. Valant-Spaight,¹⁸ A. Warburton,¹⁸ P. Avery,¹⁹ C. Prescott,¹⁹ A. I. Rubiera,¹⁹ H. Stoeck,¹⁹ J. Yelton,¹⁹ G. Brandenburg,²⁰ A. Ershov,²⁰ Y. S. Gao,²⁰ D. Y.-J. Kim,²⁰ R. Wilson,²⁰ T. Bergfeld,²¹ B. I. Eisenstein,²¹ J. Ernst,²¹ G. E. Gladding,²¹ G. D. Gollin,²¹ R. M. Hans,²¹ E. Johnson,²¹ I. Karliner,²¹ M. A. Marsh,²¹ M. Palmer,²¹ C. Plager,²¹ C. Sedlack,²¹ M. Selen,²¹ J. J. Thaler,²¹ J. Williams,²¹ K. W. Edwards,²² R. Janicek,²³ P. M. Patel,²³ A. J. Sadoff,²⁴ R. Ammar,²⁵ A. Bean,²⁵ D. Besson,²⁵ X. Zhao,²⁵ S. Anderson,²⁶ V. V. Frolov,²⁶ Y. Kubota,²⁶ S. J. Lee,²⁶ R. Mahapatra,²⁶ J. J. O'Neill,²⁶ R. Poling,²⁶ T. Riehle,²⁶ A. Smith,²⁶ C. J. Stepaniak,²⁶ J. Urheim,²⁶ S. Ahmed,²⁷ M. S. Alam,²⁷ S. B. Athar,²⁷ L. Jian,²⁷ L. Ling,²⁷ M. Saleem,²⁷ S. Timm,²⁷ and F. Wappler²⁷

(CLEO Collaboration)

¹Ohio State University, Columbus, Ohio 43210

²University of Oklahoma, Norman, Oklahoma 73019

³Purdue University, West Lafayette, Indiana 47907

⁴University of Rochester, Rochester, New York 14627

⁵Stanford Linear Accelerator Center, Stanford University, Stanford, California 94309

⁶Southern Methodist University, Dallas, Texas 75275

⁷Syracuse University, Syracuse, New York 13244

⁸University of Texas, Austin, Texas 78712

⁹University of Texas–Pan American, Edinburg, Texas 78539

¹⁰Vanderbilt University, Nashville, Tennessee 37235

¹¹Virginia Polytechnic Institute and State University, Blacksburg, Virginia 24061

¹²Wayne State University, Detroit, Michigan 48202

¹³California Institute of Technology, Pasadena, California 91125

¹⁴University of California–San Diego, La Jolla, California 92093

¹⁵University of California, Santa Barbara, California 93106

¹⁶Carnegie Mellon University, Pittsburgh, Pennsylvania 15213

¹⁷University of Colorado, Boulder, Colorado 80309-0390

¹⁸Cornell University, Ithaca, New York 14853

¹⁹University of Florida, Gainesville, Florida 32611

²⁰Harvard University, Cambridge, Massachusetts 02138

²¹University of Illinois, Urbana-Champaign, Illinois 61801

²²Carleton University, Ottawa, Ontario, Canada K1S 5B6

and the Institute of Particle Physics, Canada

²³McGill University, Montréal, Québec, Canada H3A 2T8

and the Institute of Particle Physics, Canada

²⁴Ithaca College, Ithaca, New York 14850

²⁵University of Kansas, Lawrence, Kansas 66045

²⁶University of Minnesota, Minneapolis, Minnesota 55455

²⁷State University of New York at Albany, Albany, New York 12222

(Received 2 October 2000)

The τ decays to six-pion final states have been studied with the CLEO detector at the Cornell Electron Storage Ring. The measured branching fractions are $\mathcal{B}(\tau^- \rightarrow 2\pi^- \pi^+ 3\pi^0 \nu_\tau) = (2.2 \pm 0.3 \pm 0.4) \times 10^{-4}$ and $\mathcal{B}(\tau^- \rightarrow 3\pi^- 2\pi^+ \pi^0 \nu_\tau) = (1.7 \pm 0.2 \pm 0.2) \times 10^{-4}$. A search for substructure in these decays shows that they are saturated by intermediate states with η or ω mesons. We present the first observation of the decay $\tau^- \rightarrow 2\pi^- \pi^+ \omega \nu_\tau$ and the branching fraction is measured to be $(1.2 \pm 0.2 \pm 0.1) \times 10^{-4}$. The measured branching fractions are in good agreement with the isospin expectations but somewhat below the conserved-vector-current predictions.

DOI: 10.1103/PhysRevLett.86.4467

PACS numbers: 13.35.Dx, 14.60.Fg

The decays of the τ lepton provide a good test of the standard model predictions for the hadronic weak current. The six-pion branching fractions are related to the isovector part of the e^+e^- annihilation cross section by the conserved-vector-current (CVC) hypothesis. Isospin symmetry relates the relative branching fractions of the decays $\tau^- \rightarrow 2\pi^- \pi^+ 3\pi^0 \nu_\tau$, $\tau^- \rightarrow 3\pi^- 2\pi^+ \pi^0 \nu_\tau$, and $\tau^- \rightarrow \pi^- 5\pi^0 \nu_\tau$. Therefore, the study of six-pion decays can be used to test the CVC hypothesis and isospin predictions. A better understanding of the resonance substructure in the decays is also of particular interest because of the potential application in suppressing the hadronic background in the measurement of the τ neutrino mass. In this Letter, we present a study of the decays [1] $\tau^- \rightarrow 2\pi^- \pi^+ 3\pi^0 \nu_\tau$ and $\tau^- \rightarrow 3\pi^- 2\pi^+ \pi^0 \nu_\tau$. This includes measurements of the branching fractions and the search for resonance substructure. The latter results are used to identify the vector and axial-vector current contributions to the inclusive branching fractions and allow the proper comparison of the results with the CVC and isospin symmetry predictions.

The data used in this analysis were collected with the CLEO detector [2] at the Cornell Electron Storage Ring (CESR) at center-of-mass energy of 10.6 GeV. The sample corresponds to a total integrated luminosity 13.5 fb^{-1} and contains $12.3 \times 10^6 \tau^+ \tau^-$ events [3].

For the decay $\tau^- \rightarrow 2\pi^- \pi^+ 3\pi^0 \nu_\tau$ ($3\pi^- 2\pi^+ \pi^0 \nu_\tau$), we select events with four (six) charged tracks and zero net charge. The momentum of each track must be greater than 100 MeV, and the polar angle θ of each track with respect to the beam must satisfy $|\cos\theta| < 0.90$. The track must be consistent with originating from the e^+e^- interaction point. This vertex requirement also suppresses the background from τ events with a K_S or photon conversion. The K_S background is further reduced by rejecting events containing a detached vertex with a $\pi^+ \pi^-$ mass consistent with the nominal K_S mass.

We define two exclusive sets of photon candidates in the barrel calorimeter ($|\cos\theta| < 0.80$): high quality (HQ) and low quality (LQ) photons. The selection criteria for HQ photons are designed to minimize the contamination of fake showers from hadronic interactions, while the acceptance of LQ photons ensures high event detection efficiency. A HQ photon must have an energy $E_\gamma > 120$ MeV and a lateral profile of energy deposition consistent with that expected for a photon. The Fisher discriminant technique [4] is used to differentiate a real photon from a fake photon. The discriminant function is a linear

combination of the energy of the shower and its distance to the intersection of the nearest charged track with the calorimeter surface. We use Monte Carlo simulated events (see below) to obtain the discriminant function that maximizes the separation between real and fake photons. A LQ photon is defined as a shower that does not pass the HQ photon requirements but has $E_\gamma > 30$ MeV. The Fisher discriminant for differentiating a real photon from a fake photon is used only in the decay $\tau^- \rightarrow 2\pi^- \pi^+ 3\pi^0 \nu_\tau$ due to the higher photon multiplicity. HQ photons in the end-cap calorimeter ($0.80 < |\cos\theta| < 0.95$) are selected as in the barrel.

Each event is divided into two hemispheres using the plane perpendicular to the thrust axis [5], calculated using both charged tracks and photons. There must be one charged track in one hemisphere (tag) recoiling against three or five charged tracks in the other hemisphere (signal), depending on the decay mode.

In the tag hemisphere, the total invariant mass of charged tracks and photons must satisfy $M_{\text{tag}} < 0.5$ GeV. In the signal hemisphere, there should be at least six (two) photons forming three (one) π^0 candidates for the decay $\tau^- \rightarrow 2\pi^- \pi^+ 3\pi^0 \nu_\tau$ ($3\pi^- 2\pi^+ \pi^0 \nu_\tau$). The π^0 candidates are reconstructed from photon pairs in the barrel calorimeter. All HQ photons in the barrel must be used in the reconstruction, and no HQ photon in the end cap is allowed. In case of multiple entries, we select the photon combination with smallest $\chi^2 = \sum_{i=1}^{3(1)} [S_{\gamma\gamma}^2]_i$, where $S_{\gamma\gamma} = (m_{\gamma\gamma} - m_{\pi^0})/\sigma_{\gamma\gamma}$ ($\sigma_{\gamma\gamma}$ is the mass resolution calculated from the energy and angular resolution of each photon). The signal region for the π^0 candidates is defined as $-3.5 < S_{\gamma\gamma} < 2.5$. In the case of $\tau^- \rightarrow 3\pi^- 2\pi^+ \pi^0 \nu_\tau$, we use sideband subtraction to estimate the fake π^0 background. The total invariant mass of the hadronic system in the signal hemisphere must satisfy $M_{6\pi} < M_\tau = 1.777$ GeV [6]. The signal hemisphere must have a positive pseudoneutrino mass [7]. The background from τ decays with Dalitz π^0 decays or photon conversion in inner detector material is suppressed by requiring that any pairs of oppositely charged tracks have invariant mass exceeding 120 MeV when at least one of the pair is identified as an electron and assigning the electron mass to both tracks. Two-photon backgrounds are eliminated by requiring the direction of the missing momentum of the event to satisfy $|\cos\theta_{\text{missing}}| < 0.9$.

The detection efficiency and τ migration background are calculated with a Monte Carlo technique. We

TABLE I. Summary of the results for $\tau^- \rightarrow 2\pi^- \pi^+ 3\pi^0 \nu_\tau$ and $\tau^- \rightarrow 3\pi^- 2\pi^+ \pi^0 \nu_\tau$. All errors are statistical, except the second errors in the branching fractions, which are systematic.

Decay mode	$2\pi^- \pi^+ 3\pi^0 \nu_\tau$	$3\pi^- 2\pi^+ \pi^0 \nu_\tau$
Data (events)	139.0 ± 11.8	231.0 ± 18.8
$q\bar{q}$ bg (events)	15.1 ± 3.1	25.8 ± 5.9
τ bg (events)	35.2 ± 3.4	19.4 ± 5.5
Efficiency (%)	1.65 ± 0.03	4.45 ± 0.06
\mathcal{B} (10^{-4})	$2.2 \pm 0.3 \pm 0.4$	$1.7 \pm 0.2 \pm 0.2$

use the KORALB/TAUOLA program [3] for the τ event simulation. The decay $\tau^- \rightarrow 2\pi^- \pi^+ 3\pi^0 \nu_\tau$ is modeled using a mixture of $\tau^- \rightarrow 2\pi^- \pi^+ \eta \nu_\tau$, $\tau^- \rightarrow \pi^- 2\pi^0 \eta \nu_\tau$, and $\tau^- \rightarrow \pi^- 2\pi^0 \omega \nu_\tau$. The other decay $\tau^- \rightarrow 3\pi^- 2\pi^+ \pi^0 \nu_\tau$ is modeled using a mixture of $\tau^- \rightarrow 2\pi^- \pi^+ \eta \nu_\tau$ and $\tau^- \rightarrow 2\pi^- \pi^+ \omega \nu_\tau$. The relative mixtures are determined from the measured branching fractions presented in this and a previous Letter [8]. We assume that the $3\pi\eta$ decays proceed through πf_1 with a spectral function dominated by the form factor of the $a_1(1260)$ resonance [9]. The $3\pi\omega$ system is modeled assuming dominance of the $\rho(1700)$ resonance. The

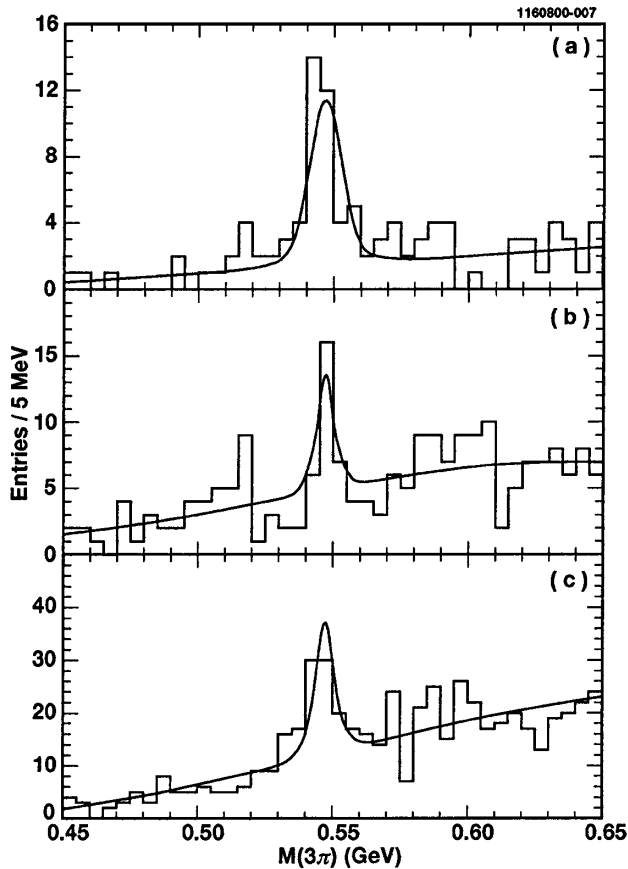


FIG. 1. Three-pion mass spectra of η candidates: (a) $M_{3\pi^0}$ in $\tau^- \rightarrow 2\pi^- \pi^+ 3\pi^0 \nu_\tau$, (b) $M_{\pi^+ \pi^- \pi^0}$ in $\tau^- \rightarrow 2\pi^- \pi^+ 3\pi^0 \nu_\tau$, (c) $M_{\pi^+ \pi^- \pi^0}$ in $\tau^- \rightarrow 3\pi^- 2\pi^+ \pi^0 \nu_\tau$. There are six entries per event in (b) and (c). The solid lines shows fits to the data.

detector response is simulated using the GEANT program [10]. The hadronic background is calculated empirically using a sample of high-mass tagged events. The signal, background, and detection efficiency are summarized in Table I. The τ background includes the decays with $K_S \rightarrow \pi^+ \pi^-$ and $\pi^0 \pi^0$.

The six-pion τ decays can proceed through the η or ω intermediate hadronic states. Figure 1 shows the invariant mass spectra of 3π combinations in the η mass region. To improve the resolution, the π^0 candidates have been kinematically constrained to the nominal π^0 mass. In the search for $\eta \rightarrow \pi^+ \pi^- \pi^0$ and $\omega \rightarrow \pi^+ \pi^- \pi^0$, we reduce the combinatoric background by rejecting events with $3\pi^0$ invariant mass within 20 MeV ($\sim 3\sigma$) of the nominal η mass. There are clear enhancements at the η mass in all three spectra. The invariant mass spectra of 3π combinations in the ω mass region are shown in Fig. 2. There is also a clear signal at the ω mass. In particular, the decay $\tau^- \rightarrow 2\pi^- \pi^+ \omega \nu_\tau$ is observed for the first time.

The η and ω signals are extracted by maximum likelihood fits with a dual Gaussian over a polynomial background. The peaks and widths of the signal mass spectra have been constrained to the Monte Carlo expectations. The results are summarized in Tables II and III.

There are several sources of systematic errors. These include the uncertainty in the number of produced $\tau^+ \tau^-$ pairs (1.4%), charged track reconstruction (1% per track), π^0 reconstruction (4% per π^0), efficiency (1%–5%), and τ migration background (4%–12%) estimates due to limited Monte Carlo statistics, hadronic background

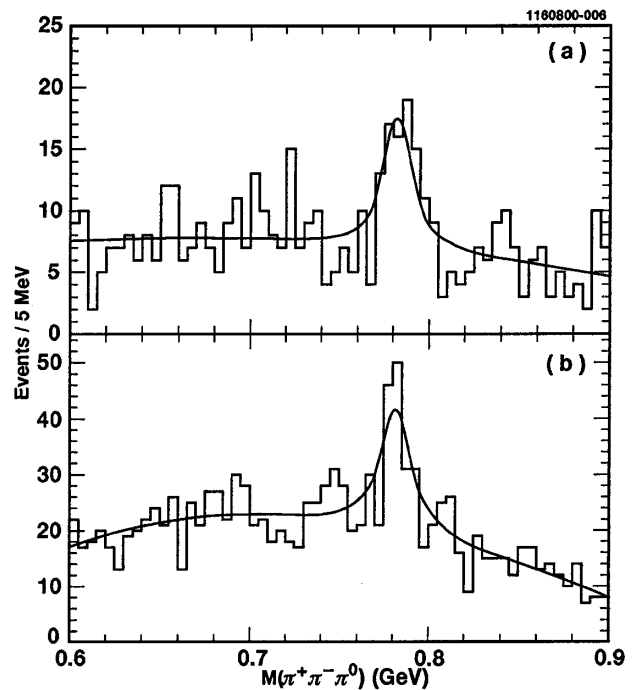


FIG. 2. Three-pion mass spectra of ω candidates (six entries per event) in (a) $\tau^- \rightarrow 2\pi^- \pi^+ 3\pi^0 \nu_\tau$ and (b) $\tau^- \rightarrow 3\pi^- 2\pi^+ \pi^0 \nu_\tau$. The solid lines shows fits to the data.

TABLE II. Summary of the results for the intermediate states with an η meson. All errors are statistical, except the second errors in the branching fractions, which are systematic.

Decay mode	$2\pi^- \pi^+ \eta \nu_\tau$ $\eta \rightarrow 3\pi^0$	$\pi^- 2\pi^0 \eta \nu_\tau$ $\eta \rightarrow \pi^+ \pi^- \pi^0$	$2\pi^- \pi^+ \eta \nu_\tau$ $\eta \rightarrow \pi^+ \pi^- \pi^0$
Data (events)	32.1 ± 6.7	15.4 ± 5.4	48.6 ± 10.2
$q\bar{q}$ bg (events)	1.9 ± 1.5	$0.2^{+1.0}_{-0.2}$	5.2 ± 3.2
τ bg (events)	0.9 ± 0.9	2.3 ± 1.6	2.5 ± 2.2
Efficiency (%)	1.28 ± 0.05	1.48 ± 0.05	4.18 ± 0.08
\mathcal{B} (10^{-4})	$2.9 \pm 0.7 \pm 0.5$	$1.5 \pm 0.6 \pm 0.3$	$1.7 \pm 0.4 \pm 0.3$

estimates (4%–9%), mixtures of various intermediate states (1%–6%), and branching fractions of $\eta \rightarrow 3\pi^0$ and $\pi^+ \pi^- \pi^0$ and $\omega \rightarrow \pi^+ \pi^- \pi^0$ [6]. For the extraction of ω and η signals, there are also systematic errors (5%–10%) resulting from the choice of combinatorial background shape and fit region. The branching fractions with systematic errors are listed in Tables I–III. The results represent significant improvement in precision over previous measurements [6,11]. The branching fractions for the two decays with ω in the final states are somewhat smaller than the recent calculations by Gao and Li [12], $\mathcal{B}(\tau^- \rightarrow \pi^- 2\pi^0 \omega \nu_\tau) = \mathcal{B}(\tau^- \rightarrow 2\pi^- \pi^+ \omega \nu_\tau) \sim 2.2 \times 10^{-4}$.

The results on the six-pion decays can be compared with the isospin symmetry and CVC predictions, after correcting for the contributions from the axial-vector current $\tau^- \rightarrow (3\pi)^- \eta \nu_\tau$, which also violates isospin conservation with the decays $\eta \rightarrow 3\pi^0$ and $\pi^+ \pi^- \pi^0$. To reduce the uncertainty in the corrections, we use measurements from these decays and the decay $\eta \rightarrow \gamma\gamma$ [8] to obtain the average branching fractions: $\bar{\mathcal{B}}(\tau^- \rightarrow 2\pi^- \pi^+ \eta \nu_\tau) = (2.3 \pm 0.5) \times 10^{-4}$ and $\bar{\mathcal{B}}(\tau^- \rightarrow \pi^- 2\pi^0 \eta \nu_\tau) = (1.5 \pm 0.5) \times 10^{-4}$. This yields the vector current branching fractions: $\mathcal{B}_V(\tau^- \rightarrow 2\pi^- \pi^+ 3\pi^0 \nu_\tau) = (1.1 \pm 0.4) \times 10^{-4}$ and $\mathcal{B}_V(\tau^- \rightarrow 3\pi^- 2\pi^+ \pi^0 \nu_\tau) = (1.2 \pm 0.2) \times 10^{-4}$, corresponding to $\sim 50\%$ and $\sim 70\%$, respectively, of the inclusive six-pion branching fractions.

The isospin model [13] classifies n -pion final states into orthogonal isospin partitions and determines their contributions to the branching fractions. The partitions are labeled by three integers (n_1, n_2, n_3) , where n_3 is the number of isoscalar subsystems of three pions, $n_2 - n_3$ is the number of isovector systems of two pions, and $n_1 - n_2$ is the

TABLE III. Summary of the results for the intermediate states with an ω meson. All errors are statistical, except the second errors in the branching fractions, which are systematic.

Decay mode	$\pi^- 2\pi^0 \omega \nu_\tau$	$2\pi^- \pi^+ \omega \nu_\tau$
Data (events)	53.1 ± 11.4	110.1 ± 18.6
$q\bar{q}$ bg (events)	$1.0^{+2.4}_{-1.0}$	$3.5^{+4.2}_{-3.5}$
τ bg (events)	8.7 ± 3.4	$2.3^{+3.7}_{-2.3}$
Efficiency (%)	1.39 ± 0.06	4.06 ± 0.14
\mathcal{B} (10^{-4})	$1.4 \pm 0.4 \pm 0.3$	$1.2 \pm 0.2 \pm 0.1$

number of single pions. For $n = 6$ there are four partitions: 510 ($4\pi\rho$), 330 (3ρ), 411 ($3\pi\omega$), and 321 ($\pi\rho\omega$), denoted according to the lowest mass states. The isospin model imposes constraints on the relative branching fractions, which can be tested by comparing the fraction,

$$f_{2\pi^- \pi^+ 3\pi^0} = \frac{\mathcal{B}_V(\tau^- \rightarrow 2\pi^- \pi^+ 3\pi^0 \nu_\tau)}{\mathcal{B}_V[\tau^- \rightarrow (6\pi)^- \nu_\tau]},$$

to a similar fraction $f_{3\pi^- 2\pi^+ \pi^0}$, where $\mathcal{B}_V[\tau^- \rightarrow (6\pi)^- \nu_\tau]$ is the sum of the branching fractions for the three six-pion vector decays. Figure 3 shows $f_{2\pi^- \pi^+ 3\pi^0}$ vs $f_{3\pi^- 2\pi^+ \pi^0}$ with our new measurement of the branching fractions. The measurement is presented as a line because $\mathcal{B}_V(\tau^- \rightarrow \pi^- 5\pi^0 \nu_\tau)$ has not been measured yet. The result is consistent with the isospin expectation since the experimental measurement overlaps with the isospin triangle. Our result indicates the 321 ($\pi\rho\omega$) partition is dominant because the decays $\tau^- \rightarrow \pi^- 2\pi^0 \omega \nu_\tau$ and $\tau^- \rightarrow 2\pi^- \pi^+ \omega \nu_\tau$ saturate the six-pion (vector) decays.

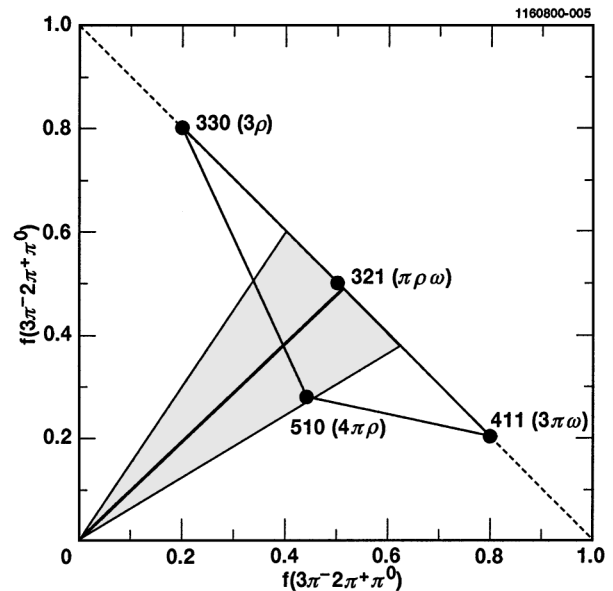


FIG. 3. Decay fractions of $\tau^- \rightarrow (6\pi)^- \nu_\tau$. The thick solid line through the origin represents the measurement. The shaded area indicates the one standard deviation region, calculated with correlated errors taken into account. The triangle bounded by the dots shows the isospin expectation.

The CVC hypothesis combined with isospin symmetry predicts that the branching fractions for both $\tau^- \rightarrow 2\pi^- \pi^+ 3\pi^0 \nu_\tau$ and $\tau^- \rightarrow 3\pi^- 2\pi^+ \pi^0 \nu_\tau$ are greater than $(2.5 \pm 0.4) \times 10^{-4}$ [14]. This is somewhat larger than the measured branching fractions for the six-pion vector decays. The discrepancy is even more significant if we compare the predicted inclusive branching fraction $\mathcal{B}_{\text{CVC}}[\tau^- \rightarrow (6\pi)^- \nu_\tau] = (12.3 \pm 1.9) \times 10^{-4}$ with the sum of the measured six-pion vector branching fractions under the assumption that $\mathcal{B}_V(\tau^- \rightarrow \pi^- 5\pi^0 \nu_\tau)$ is comparable with or smaller than $\mathcal{B}_V(\tau^- \rightarrow 2\pi^- \pi^+ 3\pi^0 \nu_\tau)$ and $\mathcal{B}_V(\tau^- \rightarrow 3\pi^- 2\pi^+ \pi^0 \nu_\tau)$ [15]. This assumption is consistent with the observation that the six-pion vector decays are saturated by intermediate states with an ω meson, which implies a small decay width for the 510 ($4\pi\rho$) state, the only state that contributes to the decay $\tau^- \rightarrow \pi^- 5\pi^0 \nu_\tau$. The discrepancy might be explained by the sizable presence of $I = 0$ states in the e^+e^- annihilation data that should be subtracted before calculating the CVC prediction.

In conclusion, the branching fraction for two six-pion decays have been measured with much improved precision. The resonance substructure in the decays has been studied. In particular, the decay $\tau^- \rightarrow 2\pi^- \pi^+ \omega \nu_\tau$ has been observed for the first time. Within the statistical precision, the decays are saturated by η and ω intermediate states. The measured branching fractions are in good agreement with the isospin expectations but somewhat below the CVC predictions.

We gratefully acknowledge the effort of the CESR staff in providing us with excellent luminosity and running conditions. This work was supported by the National Science Foundation, the U.S. Department of Energy, the Research Corporation, the Natural Sciences and Engineering Research Council of Canada, the A.P. Sloan Foundation, the Swiss National Science Foundation, the Texas Ad-

vanced Research Program, and the Alexander von Humboldt Stiftung.

*Permanent address: Massachusetts Institute of Technology, Cambridge, MA 02139.

- [1] We assume all charged particles in the final states are pions. Charge conjugate states are implied throughout this Letter.
- [2] CLEO Collaboration, Y. Kubota *et al.*, Nucl. Instrum. Methods Phys. Res., Sect. A **320**, 66 (1992); T. S. Hill, Nucl. Instrum. Methods Phys. Res., Sect. A **418**, 32 (1998).
- [3] S. Jadach and Z. Was, Comput. Phys. Commun. **36**, 191 (1985); **64**, 267 (1991); S. Jadach, J. H. Kuhn, and Z. Was, *ibid.* **64**, 275 (1991).
- [4] See, for example, L. Lebart, A. Morineau, and K. Warwick, *Multivariate Descriptive Statistical Analysis* (Wiley, New York, 1984).
- [5] E. Farhi, Phys. Rev. Lett. **39**, 1587 (1977).
- [6] Particle Data Group, D. E. Groom *et al.*, Eur. Phys. J. C **3**, 1 (1998).
- [7] CLEO Collaboration, D. Gibaut *et al.*, Phys. Rev. Lett. **73**, 934 (1994).
- [8] CLEO Collaboration, T. Bergfeld *et al.*, Phys. Rev. Lett. **79**, 2406 (1997).
- [9] B. A. Li, Phys. Rev. D **55**, 1436 (1997).
- [10] R. Burn *et al.*, CERN Report No. CERN-DD/EE/84-1, 1987 (unpublished).
- [11] The results presented in this Letter supercede our previous results in Ref. [7] and CLEO Collaboration, S. Anderson *et al.*, Phys. Rev. Lett. **79**, 3814 (1997).
- [12] J. Gao and B. A. Li, hep-ph/0004097.
- [13] A. Pais, Ann. Phys. (Paris) **9**, 548 (1960).
- [14] S. I. Eidelman and V. N. Ivanchenko, Nucl. Phys. B (Proc. Suppl.) **55**, 181 (1997).
- [15] Isospin symmetry imposes the constraint $\mathcal{B}_V(\tau^- \rightarrow \pi^- 5\pi^0 \nu_\tau) \leq (9/26)[\mathcal{B}_V(\tau^- \rightarrow 2\pi^- \pi^+ 3\pi^0 \nu_\tau) + \mathcal{B}_V(\tau^- \rightarrow 3\pi^- 2\pi^+ \pi^0 \nu_\tau)]$.